

Assessment of lung function using a non-invasive oscillating gas-forcing technique[☆]

Lei Clifton^{a,b,*}, David A. Clifton^b, Clive E.W. Hahn^a, Andrew D. Farmery^a

^a Nuffield Division of Anaesthetics, Nuffield Department of Clinical Neurosciences, University of Oxford, John Radcliffe Hospital, Oxford OX3 9DU, UK

^b Institute of Biomedical Engineering, Department of Engineering Science, University of Oxford, Old Road Campus, Roosevelt Drive, Oxford OX3 7DQ, UK

ARTICLE INFO

Article history:

Accepted 13 May 2013

Keywords:

Lung function
Non-invasive
Alveolar volume
Airway dead space
Pulmonary blood flow
Tidal ventilation
Model
Oscillating
Gas-forcing
Nitrous oxide
Oxygen
Indicator gas

ABSTRACT

Conventional methods for monitoring lung function can require complex, or special, gas analysers, and may therefore not be practical in clinical areas such as the intensive care unit (ICU) or operating theatre. The system proposed in this article is a compact and non-invasive system for the measurement and monitoring of lung variables, such as alveolar volume, airway dead space, and pulmonary blood flow. In contrast with conventional methods, the compact apparatus and non-invasive nature of the proposed method could eventually allow it to be used in the ICU, as well as in general clinical settings. We also propose a novel tidal ventilation model using a non-invasive oscillating gas-forcing technique, where both nitrous oxide and oxygen are used as indicator gases. Experimental results are obtained from healthy volunteers, and are compared with those obtained using a conventional continuous ventilation model. Our findings show that the proposed technique can be used to assess lung function, and has several advantages over conventional methods such as compact and portable apparatus, easy usage, and quick estimation of cardiopulmonary variables.

© 2013 The Authors. Published by Elsevier B.V. All rights reserved.

1. Introduction

Patients in the intensive care unit (ICU) often require mechanical ventilatory support using positive pressure ventilation (Rouby et al., 2004). Estimation of lung variables benefits these patients because they help the clinician to determine the most suitable values in therapeutic measures such as positive end-expired pressure (PEEP). They could also help to avoid the common problem of ventilator induced lung injury (VILI). Three key lung variables are:

1. alveolar volume at the end of an expiration, V_A
2. airway dead space volume, V_D
3. pulmonary blood flow, \dot{Q}_p

Current techniques for measuring these variables can require the cooperation of the patient, or a modification of the patient's

ventilator system. ICU patients depend on complex life support and monitoring equipment, and thus are usually unable to cooperate with the physician. These patients are therefore some of the most difficult to assess using conventional lung function tests.

Zwart et al. pioneered the non-invasive oscillating gas-forcing technique (Zwart et al., 1976, 1978), and used halothane as the forcing gas at a very low concentration (around 0.02, v/v) to measure the average ventilation-perfusion ratio (\dot{V}/\dot{Q}) in the lung. Hahn et al. further developed this method by using biologically inert gases such as nitrous oxide (N_2O) and argon (instead of halothane) to measure V_A , V_D , and \dot{Q}_p non-invasively (Hahn et al., 1993; Williams et al., 1994). They later proposed that oxygen (O_2) can be used to measure V_A and V_D (Hahn, 1996; Hamilton, 1998). When O_2 was used together with N_2O , their model can also be used to measure \dot{Q}_p . However, their initial technique required a respiratory mass spectrometer that presented considerable difficulty when used in the ICU due to its size, noise, complexity, high maintenance requirements, and lack of portability (Farmery, 2008). Moreover, their prototype gas mixer is not compatible with modern ICU ventilators. There was therefore a clinical need to design a new system to deliver indicator gases according to the patient's breathing flow rates in real time.

A conventional existing model based on continuous ventilation is described in Section 2; we propose a novel non-invasive method for estimating the cardiopulmonary variables, V_A , V_D , and \dot{Q}_p in Section 3. Indicator gases O_2 and N_2O are injected into the patient's

[☆] This is an open-access article distributed under the terms of the Creative Commons Attribution-NonCommercial-No Derivative Works License, which permits non-commercial use, distribution, and reproduction in any medium, provided the original author and source are credited.

* Corresponding author at: Institute of Biomedical Engineering, Department of Engineering Science, University of Oxford, Old Road Campus, Roosevelt Drive, Oxford OX3 7DQ, UK. Tel.: +44 01865 617670.

E-mail addresses: lei.clifton@eng.ox.ac.uk (L. Clifton), david.clifton@eng.ox.ac.uk (D.A. Clifton), clive.hahn@ndcn.ox.ac.uk (C.E.W. Hahn), andrew.farmery@ndcn.ox.ac.uk (A.D. Farmery).

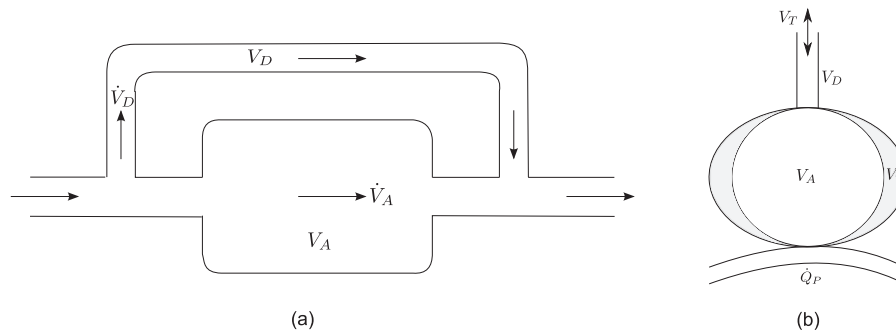


Fig. 1. Schematic diagrams for a continuous ventilation model and the breath-by-breath “balloon-on-a-straw” tidal ventilation model, shown in (a) and (b), respectively. Whereas the traditional continuous ventilation model regards the lung as a box of a rigid volume with a continuous flow passing through it, and a parallel dead space also with a continuous flow, the tidal ventilation model, has a volume V_A at the end of an expiration and which expands to volume $V_A + V_T$ at the end of an inspiration. The inspired gas enters the dead space of volume V_D before entering the lung, and the expired gas travels through the dead space before entering the mouth. Gas enters and leaves the lung at flow rate $\dot{V}(t)$ at time t .

airway breath-by-breath “on the fly” to make the concentration of these gases vary sinusoidally in the inspired gas. The apparatus is compact in size and is portable, consisting of a flow rate sensor, a gas concentration sensor, and two mass flow controllers (MFCs). We improve the original Bohr equation for dead space calculation in Section 4. Results obtained using the proposed single alveolar compartment tidal ventilation model are compared with those obtained using the continuous ventilation model in Section 5. A discussion is presented in Section 6, and conclusions are drawn in Section 7. A list of abbreviations can be found in the appendix.

2. The continuous ventilation model

The continuous ventilation model (Zwart et al., 1976; Hahn et al., 1993; Hahn, 1996; Williams et al., 1994), as shown in Fig. 1(a), treats the lung as a rigid volume with a constant and continuous flow passing through it. Dead space is regarded as a tube of negligible volume parallel to the lung, with another constant flow passing through it. The inspired concentration of an indicator gas $F_I(t)$ is controlled by a gas mixing apparatus, and is forced to vary sinusoidally at a chosen frequency.

$$F_I(t) = M_I + \Delta F_I \sin(2\pi f t + \phi), \quad (1)$$

where M_I and ΔF_I are the mean and amplitude of the forcing indicator gas sinusoid, respectively, f is the forcing frequency in min^{-1} , and ϕ is the phase of the sine wave.

In the absence of venous recirculation, and assuming that the inspired indicator gas concentration is in equilibrium in all tissues throughout the respiratory and cardiovascular systems, the mixed-expired and end-expired (i.e., alveolar) indicator gas concentrations are also forced to be sinusoidal (Zwart et al., 1976; Hahn et al., 1993; Williams et al., 1994).

Let F_A be the indicator gas concentration in the alveolar compartments of the lung, and ΔF_A be the amplitude of F_A measured from its mean; we therefore have (Hahn et al., 1993)

$$\frac{\Delta F_A}{\Delta F_I} = \frac{1}{\sqrt{(1 + \lambda_b(\dot{Q}_P/\dot{V}_A))^2 + \omega^2 \tau^2}} \quad (2)$$

in which λ_b is the blood-gas solubility coefficient; note that $\lambda_b = 0.03$ for O_2 , and $\lambda_b = 0.47$ for N_2O . ω is the forcing frequency in radians; i.e., $\omega = 2\pi f$. τ is the lung ventilatory time constant,

$$\tau = \frac{V'_A}{\dot{V}_A}, \quad (3)$$

where V'_A is the *effective* lung volume given by (4) below, and \dot{V}_A is the ventilation rate in L/min (Gavaghan and Hahn, 1995). The relationship is given by

$$V'_A = V_A + \lambda_b V_{bl} + \lambda_{tl} V_{tl}, \quad (4)$$

where V_{bl} is the volume of blood in the lung, V_{tl} is the volume of lung tissue, and λ_{tl} is the lung tissue-gas partition coefficient. Indicator gas O_2 can be approximately regarded as a non-soluble gas with $\lambda_b \approx 0$ and $\lambda_{tl} \approx 0$, hence $V'_A = V_A$. Therefore, τ for O_2 is

$$\tau_{\text{O}_2} \approx \frac{V_A}{\dot{V}_A}, \quad (5)$$

For the soluble gas N_2O , using the values of the above variables given in Gavaghan and Hahn (1995), (4) can be re-written as $V'_A = V_A + 0.43$. Therefore τ for N_2O is

$$\tau_{\text{N}_2\text{O}} = \frac{V_A + 0.43}{\dot{V}_A}. \quad (6)$$

We can express the ventilation rate \dot{V}_A by (Williams et al., 1994)

$$\dot{V}_A = R(V_T - V_D), \quad (7)$$

where R is the respiration rate in breaths/min, V_T is the tidal volume, and V_D is the airway dead space volume.

At high frequencies ω , the term $\omega^2 \tau^2$ dominates the denominator in (2), therefore allowing τ to be estimated using

$$\frac{\Delta F_A}{\Delta F_I} \rightarrow \frac{1}{\omega \tau}, \quad (8)$$

where ΔF_A , ΔF_I , and ω are known values. The estimated τ is then subsequently used to determine lung volume V_A using (3) and (4).

Conversely, at low values of ω , the term $\lambda_b \frac{\dot{Q}_P}{\dot{V}_A}$ dominates the denominator in (2), and therefore reveals information concerning \dot{Q}_P . This indicates that careful selection of ω allows the variable determination of both lung volume V_A and lung perfusion \dot{Q}_P .

Hahn et al. (1993) found that the forcing sinusoidal frequency should be $f > 1$ min, when N_2O is used as the forcing gas.

Lung volume V_A derived from a continuous ventilation model is greater than the actual V_A , due to the assumption that V_A is constant. In reality, the lung volume including dead space volume V_D varies tidally between $(V_A + V_D)$ at the beginning of inspiration and $(V_A + V_D + V_T)$ at the end of inspiration. Sainsbury et al. (1997) showed that subtracting a correction term V_c from the lung volume determined by the continuous ventilation model produces a more realistic estimate of the lung volume,

$$V_c = \frac{1}{2}(V_T + V_D) \quad (9)$$

In our proposed new system, we have used both O₂ and N₂O to estimate V_A and \dot{Q}_P . With the indicator gas O₂ regarded as a non-soluble gas with $\lambda_b \approx 0$, (2) therefore becomes

$$\left(\frac{\Delta F_A}{\Delta F_I}\right)_{O_2} = \frac{1}{\sqrt{1 + \omega^2 \tau_{O_2}^2}}, \quad (10)$$

where $(\Delta F_A/\Delta F_I)_{O_2}$ indicates $\Delta F_A/\Delta F_I$ obtained using O₂ data.

From (5) and (10), we have

$$V_A = \frac{\dot{V}_A T}{2\pi} \left[\left(\frac{\Delta F_A}{\Delta F_I}\right)_{O_2}^{-2} - 1 \right]^{1/2} \quad (11)$$

where \dot{V}_A is given by (7), and T is the forcing sinusoidal period in minutes; i.e., $T = f^{-1} = 2\pi(\omega)^{-1}$. Here we have reached the estimate of lung volume V_A , using (11).

For the soluble indicator gas N₂O, (2) can be re-written as

$$\left(\frac{\Delta F_A}{\Delta F_I}\right)_{N_2O} = \frac{1}{\sqrt{(1 + 0.47(\dot{Q}_P/\dot{V}_A))^2 + \omega^2 \tau_{N_2O}^2}} \quad (12)$$

From (5), (6), (10) and (12), we have

$$\dot{Q}_P = \frac{\dot{V}_A}{0.47} \left\{ \left[\left(\frac{\Delta F_A}{\Delta F_I}\right)_{N_2O}^{-2} - \left(\frac{V_A + 0.43}{V_A}\right)^2 \cdot \left(\frac{\Delta F_A}{\Delta F_I}\right)_{O_2}^{-2} + \left(\frac{V_A + 0.43}{V_A}\right)^2 \right]^{1/2} - 1 \right\}, \quad (13)$$

where \dot{V}_A is given by (7), and V_A is given by (11).

A set of V_A and \dot{Q}_P can be produced at any sinusoidal period T , using (11) and (13) where both O₂ and N₂O contribute to the estimation.

In previous work concerning the continuous ventilation model (Hahn, 1996; Hamilton, 1998), only one type of indicator gas was used, hence V_A and \dot{Q}_P had to be estimated separately. One contribution of the proposed system is that, for the first time, V_A and \dot{Q}_P can be estimated at the same time using the continuous ventilation model, and this therefore reduces the time to obtain estimates V_A and \dot{Q}_P . This is achieved by injecting two types of indicator gases O₂ and N₂O simultaneously, where O₂ data are used to estimate V_A , and N₂O data are used to estimate \dot{Q}_P , when the continuous ventilation model is applied.

A drawback of the continuous ventilation model is that it requires a relatively long period of time to obtain its measurements, mainly because obtaining $\Delta F_A/\Delta F_I$ requires the duration of signals to be at least one period T (and is typically taken to be several periods). In the ICU or operating theatre where prompt response to changes in patient conditions is required, it is essential to estimate patient lung function in a short time. In Section 3, we propose a breath-by-breath tidal ventilation model (assuming a single alveolar compartment), which allows fast estimation of patient lung function in a non-invasive manner.

3. The tidal ventilation model

3.1. A breath-by-breath model

In contrast with the continuous ventilation model discussed in Section 2, a tidal ventilation model was introduced by Gavaghan and Hahn (1996), and later modified by Williams et al. (Williams et al., 1998; Whiteley et al., 2000, 2003; Farmery, 2008). We employ a “balloon-on-a-straw” tidal ventilation model (Hahn and Farmery, 2003), shown in Fig. 1(b).

In a “balloon-on-a-straw” tidal ventilation model, the gases enter and leave the lung via a common dead space (the straw) of volume V_D . Compared with the rigid volume of the continuous ventilation model, the lung volume (the balloon) in the “balloon-on-a-straw” model reflects the reality of breathing, where the

lung expands during inspiration and empties during expiration. A detailed description of the “balloon-on-a-straw” tidal ventilation model can be found in Hahn and Farmery (2003).

Let $F_{A,n}$ be the indicator gas concentration in the lung during breath n ; we assume that $F_{A,n}$ is constant during any breath n , and hence is not dependent on time t . The volumes of the indicator gas at the end of breath $(n-1)$ and n are $V_A F_{A,n-1}$ and $V_A F_{A,n}$, respectively. Let \mathcal{V}_I be the volume of indicator gas delivered into the lung during breath n , let \mathcal{V}_E be the expired volume of the indicator gas during breath n , and let \mathcal{V}_Q be the uptake of the indicator gas (i.e., the amount of indicator gas absorbed by the pulmonary capillary blood in the lung) during breath n . Conservation of mass requires that at the end of breath n , the volume change of indicator gas in the alveolar compartments is equal to the inspired indicator gas less the sum of expired volume and the pulmonary uptake. Hence,

$$V_A F_{A,n} - V_A F_{A,n-1} = \mathcal{V}_I - \mathcal{V}_E - \mathcal{V}_Q. \quad (14)$$

In the remainder of this section, we will further explore the mathematical expression of \mathcal{V}_I , \mathcal{V}_E , and \mathcal{V}_Q .

The inspired indicator gas volume \mathcal{V}_I can be expressed as

$$\mathcal{V}_I = \int_{t_{bl}}^{t_{el}} \dot{V}(t) F_{IA,n}(t) dt \quad (15)$$

where t_{bl} is the time at the beginning of inspiration, t_{el} is the time at the end of inspiration, $\dot{V}(t)$ is the measured respiratory flow rate at time t , and $F_{IA,n}(t)$ is the inspired concentration of the indicator gas that enters the alveolar compartment during breath n .

The gas inspired into the alveolar compartment is in two parts: the first comes from the dead space compartment, and the second is fresh inspired gas. $F_{IA,n}(t)$ also therefore consists of two parts: the first part has a value of $F_{A,n-1}$ since this was the alveolar concentration of indicator gas from the previous breath which now resides in the dead space; the second part has a value of $F_{I,n}(t)$, the concentration of the indicator gas measured by the concentration sensor at the mouth during inspiration of breath n . Here we have made the distinction between indicator gas concentration *in the lung* and that *at the mouth*, and therefore $F_{IA,n}(t)$ can be expressed as

$$F_{IA,n}(t) = \begin{cases} F_{A,n-1} & \text{if } t_{bl} \leq t < t_{bl} + T_{DI} \\ F_{I,n}(t) & \text{if } t_{bl} + T_{DI} \leq t < t_{el}, \end{cases} \quad (16)$$

where T_{DI} is the time taken for the indicator gas to travel through the dead space during inspiration of breath n .

Substituting (16) into (15), we have

$$\begin{aligned} \mathcal{V}_I &= \int_{t_{bl}}^{t_{bl}+T_{DI}} \dot{V}(t) F_{A,n-1} dt + \int_{t_{bl}+T_{DI}}^{t_{el}} \dot{V}(t) F_{I,n}(t) dt \\ &= V_D F_{A,n-1} + \int_{t_{bl}}^{t_{el}-T_{DI}} \dot{V}(t) F_{I,n}(t) dt \end{aligned} \quad (17)$$

Here we have arrived at an expression for \mathcal{V}_I . Now we seek to find an expression for \mathcal{V}_E and \mathcal{V}_Q , to complete the conservation of mass equation (14).

In the above analysis of the first part of $F_{IA,n}(t)$ in (16), we have assumed that $F_{A,n}$ (the indicator gas concentration in the lung during breath n) is constant during any breath n ; this means that $F_{A,n}$ is

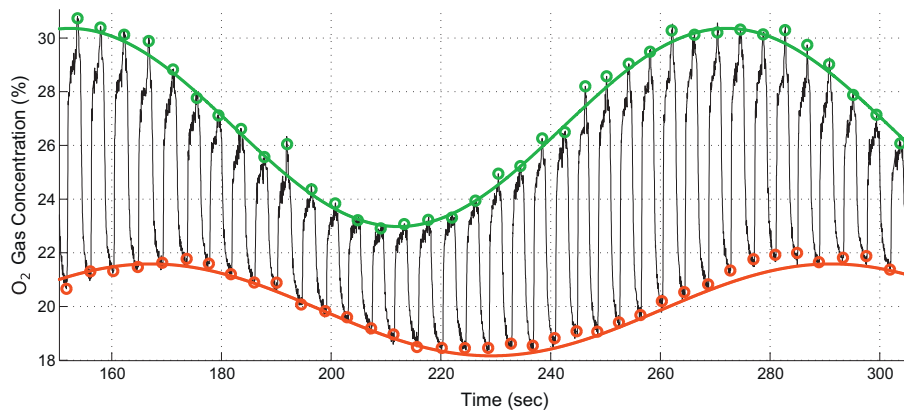


Fig. 2. Concentration of indicator gas O_2 in the airway flow of a healthy male volunteer. The forcing sinusoidal period $T = 2$ min. The green and red circles are placed where the flow signal changes its direction, indicating the end of inspiration and expiration, respectively. The green and red sinusoids are fitted to the green and red circles, respectively. The sinusoids show that the concentration of the indicator gas varies sinusoidally, at the chosen value of T .

equal to $F_{E',n}$ (the measured indicator gas concentration at the end of expiration in breath n). That is,

$$F_{A,n} = F_{E',n} \quad (18)$$

The reason for using $F_{E',n}$ here is that it is more readily measured than $F_{A,n}$. $F_{E'}$ (the function of $F_{E',n}$ over all breaths) is a sine wave expressed in Eqs. (25) and (26), using our indicator gas injection method in Section 3.2. Eq. (18) implies that F_A (the function of the indicator gas concentration in the lung from all breaths) is also a sine wave.

The expired indicator gas volume \mathcal{V}_E can be expressed as

$$\mathcal{V}_E = V_{T,n} F_{A,n}, \quad (19)$$

where $V_{T,n}$ is the tidal volume (the volume of gas inhaled and exhaled) during breath n .

Substituting (18) into (19) gives the final expression for \mathcal{V}_E

$$\mathcal{V}_E = V_{T,n} F_{E',n}. \quad (20)$$

The uptake of the indicator gas \mathcal{V}_Q is

$$\mathcal{V}_Q = \dot{Q}_p \lambda_b (F_{A,n} - F_{\bar{V},n}) T_n, \quad (21)$$

where \dot{Q}_p is the pulmonary blood flow, λ_b is blood solubility coefficient of the indicator gas, and T_n is the duration of breath n . $F_{\bar{V},n}$ is the average indicator gas concentration returned to the lung through venous recirculation in breath n .

Some of the inspired indicator gas is taken up by the pulmonary capillary blood in the lung, and eventually returns to the lung via venous recirculation. Previous research has shown that at carefully chosen forcing frequencies, the venous recirculation effects can be ignored (Hahn et al., 1993; Gavaghan and Hahn, 1995) because the oscillatory component of the venous concentration signal is negligible at these forcing frequencies, leaving

$$F_{\bar{V},n} = M_A, \quad (22)$$

where M_A is the mean of the alveolar sinusoid F_A . We have stated in (18) that M_A is equal to the mean of the measured sinusoid $F_{E'}$.

Substituting (22) and (18) into (21), we have an expression for \mathcal{V}_Q

$$\mathcal{V}_Q = \dot{Q}_p \lambda_b (F_{E',n} - M_A) T_n. \quad (23)$$

Here we have reached expressions for \mathcal{V}_I , \mathcal{V}_E , and \mathcal{V}_Q in Eqs. (17), (20) and (23), respectively. Substituting them into the right-hand-side of (14), and substituting (18) into the left-hand-side of (14),

we have

$$\begin{aligned} V_A (F_{E',n-1} - F_{E',n}) + \dot{Q}_p \lambda_b (M_A - F_{E',n}) T_n \\ = V_{T,n} F_{E',n} - \left[V_D F_{E',n-1} + \int_{t_{bl}}^{t_{el}-T_D} \dot{V}(t) F_{I,n}(t) dt \right]. \end{aligned} \quad (24)$$

This is the conservation of mass equation for the lung variables that we aim to estimate, expressed in terms of volume change of the indicator gas in a breath-by-breath manner. Our goal is to determine the values of V_A and \dot{Q}_p in (24). The measured variables are $F_{E',n-1}$, $F_{E',n}$, $F_{I,n}(t)$, $V_{T,n}$, and M_A ; the blood solubility coefficient λ_b is a known constant for the chosen indicator gas. We have previously used the Bohr equation to calculate V_D (Clifton et al., 2009); here V_D is calculated using the method proposed in Section 4 where both CO_2 and the indicator gas were used to achieve a robust estimate of V_D . Using (24), every two successive breaths produce an equation; therefore a total of N breaths results in $N - 1$ equations of two unknown values, V_A and \dot{Q}_p . For this set of $N - 1$ linear equations, we used the least-squares technique to determine the values of V_A and \dot{Q}_p .

3.2. “On the fly” indicator gas delivery

Early ventilators such as the Servo 900 (Siemens) were capable of being driven by an auxiliary low pressure gas supply, and so could be fed by a gas mixer generating sinusoidal indicator concentrations. However, modern ICU ventilators cannot be adapted easily to allow premixed gases to be delivered. Consequently, the indicator gas must be injected into the inspiratory limb of the ventilator “on the fly”. We adapted a novel on-line indicator gas delivery method (Farmery, 2008), where the indicator gas is injected into the patient’s inspiratory breathing flow and mixed in real time immediately before entering the mouth. Two types of indicator gases, O_2 and N_2O , are injected simultaneously into the patient’s airway flow during inspiration. Two mass flow controllers (MFC, Alicat Scientific, Inc., USA) were used to deliver the two indicator gases at rates proportional to the subject’s inspiratory flow rate at any instant such that the indicator concentration remained constant within the breath, but could be forced to vary between breaths according to

$$F_{N_2O}(t) = M_{N_2O} + \Delta F_{N_2O} \sin(2\pi f t) \quad (25)$$

$$F_{O_2}(t) = M_{O_2} + \Delta F_{O_2} \sin(2\pi f t), \quad (26)$$

where $F_{N_2O}(t)$ is the concentration of the injected N_2O flow; M_{N_2O} and ΔF_{N_2O} are the mean and amplitude of the forcing N_2O sinusoid,

respectively; $F_{O_2}(t)$, M_{O_2} , and ΔF_{O_2} are similar denotations for O_2 . Fig. 2 shows the resulting concentration of the indicator gas O_2 .

A *D-lite*TM flow sensor (GE Healthcare, Finland) and a differential pressure transducer (Validyne Engineering, USA) were used to measure breathing flow rates. The indicator gas concentration was measured by an *IRMA*TM multi-gas analyser (PHASEIN AB, Sweden) that measures O_2 , N_2O , CO_2 , and other anaesthetic gases simultaneously. Detailed measuring principles and sensor calibration data can be found in [Farmery \(2008\)](#) and [Van der Hoeven \(2007\)](#). Both the flow sensor and the concentration sensor can be mounted on the breathing tube connected to the patient. Compared with the apparatus for previous continuous ([Hahn et al., 1993](#); [Williams et al., 1994](#)) and tidal models ([Williams et al., 1998](#)), the proposed setup is portable, simple to use, and is suitable for the ICU because of its non-invasive approach.

It is essential to enhance the “response time” (the time taken for the signal to rise to 90% of its value after a step response) of the concentration signals in the proposed breath-by-breath tidal ventilation model ([Farmery and Hahn, 2000](#)) in order to avoid errors in estimation of the mass flux of gases. A first-order exponential model ([Clifton et al., 2009](#)) has been applied to reduce the response time to around 100 ms.

3.3. Venous recirculation

Both the continuous model ([Zwart et al., 1976, 1978](#)) and the tidal model ([Gavaghan and Hahn, 1996](#); [Williams et al., 1998](#); [Whiteley et al., 2000, 2003](#)) have regarded the oscillatory component of the venous recirculation signals as being sufficiently small to be neglected. Gavaghan et al. constructed a mathematical model including recirculation times ([Gavaghan and Hahn, 1995](#)) and concluded that the recirculation effects are negligible in the forcing period range of $0.5 \text{ min} \leq T \leq 4 \text{ min}$ for the soluble gases halothane, acetylene, and N_2O ([Gavaghan and Hahn, 1995](#)), and become more pronounced at long forcing periods $T > 4 \text{ min}$. Williams et al. recommended forcing sine periods of $2 \text{ min} \leq T \leq 3 \text{ min}$ for solving airway dead space V_D and lung volume V_A ([Williams et al., 1994, 1998](#)). In Section 5 we show that $2 \text{ min} \leq T \leq 4 \text{ min}$ is a potentially appropriate range for forcing sinusoidal periods T .

4. Dead space calculation

4.1. Original Bohr equation

Various methods for calculating the volume of airway dead space V_D are discussed in [Farmery \(2008\)](#), among which two classical methods are Fowler’s method ([Fowler, 1948](#); [Fletcher et al., 1981](#)) and the Bohr equation ([Hlastala and Berger, 1996](#)). The latter is used in the proposed method as follows:

$$V_D = V_T \frac{F_A - F_{\bar{E}}}{F_A - F_I}, \quad (27)$$

where $F_{\bar{E}}$ is the mixed expired indicator gas concentration, and F_I is the indicator gas concentration at the end of inspiration.

We have assumed that $F_{A,n}$ is constant during breath n , and is equal to $F_{E',n}$ in (18). Substituting (18) into (27) gives

$$V_D = V_T \frac{F_{E'} - F_{\bar{E}}}{F_{E'} - F_I}, \quad (28)$$

where $F_{E'}$ is the indicator gas concentration at the end of expiration. In the tidal ventilation model, each breath n produces data which allows a separate solution of the Bohr equation using (28).

However, one potential problem when (28) is used to produce an estimate of the value of V_D at each breath is that at breaths where the values of the numerator or the denominator in (28) are close to

zero, the estimates of V_D become sensitive to small measurement errors, and so the solution becomes unstable.

Another problem is the choice of gases when using (28): both CO_2 and the indicator gas produce a set of Bohr equations. The estimated values of V_D obtained using different gases are usually different from one another, and it is difficult to know which gas produces the more reliable results. A simple average of all the various estimates for each indicator gas may not be sufficiently stable, if some estimates are erroneous.

4.2. Improved Bohr equation

To overcome the problems described above, we propose a regression approach to improve the stability of the original Bohr equation. We re-write (28) as

$$(F_{E'} - F_{\bar{E}}) = \frac{V_D}{V_T} (F_{E'} - F_I). \quad (29)$$

Each breath produces a set of values for x and y , corresponding to a point on a straight line

$$y = ax, \quad (30)$$

where $y = (F_{E'} - F_{\bar{E}})$, $x = (F_{E'} - F_I)$, and a is the slope of the line, $a = V_D/V_T$. The optimal value of V_D can be determined by finding the value of a that best describes the straight line using linear regression.

Values (x, y) of both CO_2 and the indicator gas from all breaths are used in the linear regression, in order to achieve a robust estimate that incorporates results obtained using both gases. The proposed method uses all breaths without suffering from the instabilities induced by near-zero values in the original Bohr equation.

The results shown in Section 5.2 indicate that using both gases achieves a more robust estimate than using a single gas, and that the proposed linear regression approach is more stable than using a simple average of estimates obtained using the original Bohr equation.

5. Results and comparisons

Twenty data sessions from healthy human volunteers were studied, with results obtained from one volunteer studied in detail in this paper, for illustration of the prototype system. Results obtained from all volunteers are then summarised in Fig. 4 and Table 3. Both N_2O and O_2 are injected as indicator gases.

For each of $T = 2, 3, 4$, and 5 min , data were collected for 10 min duration. For the tidal ventilation model, the data were divided into 20 data windows (i.e., each window contained 30 s of data); each of these windows of data was used to estimate V_D , V_A , and \dot{Q}_p . The mean and standard deviation of these estimates are shown in Fig. 3(a)–(c). The continuous ventilation model requires measurements of ΔF_A and ΔF_I , and hence the total duration of data was used to produce a single set of estimates for this method, against which our breath-by-breath tidal ventilation model will be compared.

5.1. Comparison of the continuous ventilation model with the tidal ventilation model

As described in Section 2, for the continuous ventilation model, a set of V_A and \dot{Q}_p estimates can be produced at any sinusoidal period T , using (11) and (13), where both O_2 and N_2O estimates contribute to the overall estimates.

For the tidal ventilation model, the results obtained using N_2O are presented. The results obtained using O_2 are similar to those obtained using N_2O , and are not shown here. In (25), we have chosen indicator gas parameters $M_{N_2O} = 0.06 \text{ v/v}$, $A_{N_2O} = 0.03 \text{ v/v}$, which is a non-toxic concentration level for N_2O .

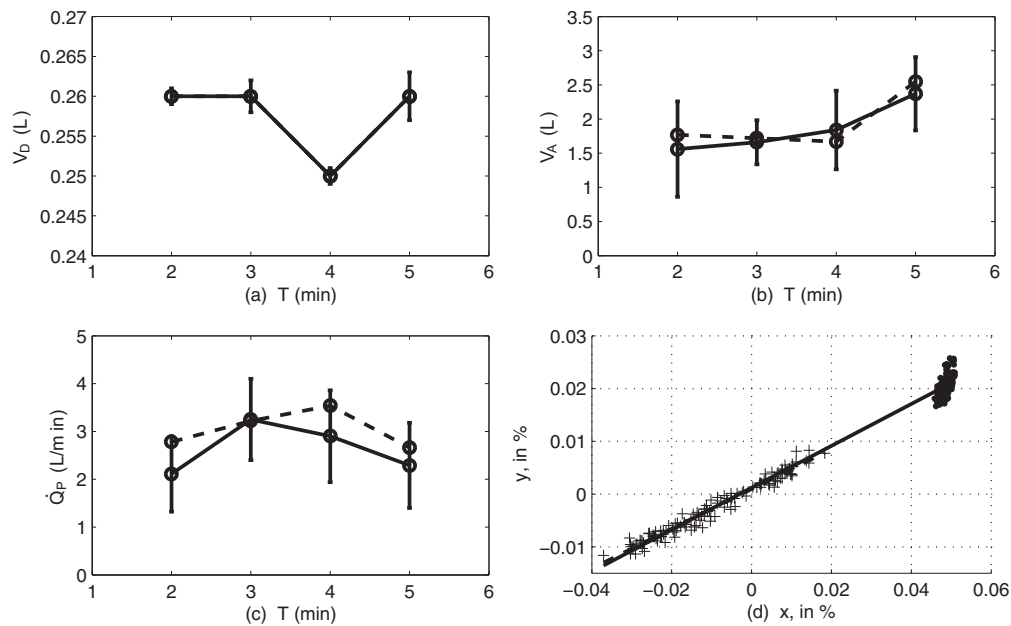


Fig. 3. (a)–(c) Comparison of results for the continuous ventilation model with those of the tidal ventilation model, at forcing sinusoidal periods $T=2, 3, 4, 5$ min for one individual. Results for the continuous and the tidal ventilation model are shown by dashed and solid lines, respectively. Note that results obtained using the continuous ventilation model do not have the error bars, because it uses all of the data to perform a single estimation. (d) Dead space results obtained using a healthy male volunteer. (x, y) pairs obtained using CO_2 and N_2O are shown using $(\cdot, +)$, respectively. Regression lines obtained using only N_2O and using both CO_2 and N_2O are shown by solid and dashed lines, respectively. The regression line obtained using N_2O is approximately the same as the regression line obtained using both CO_2 and N_2O .

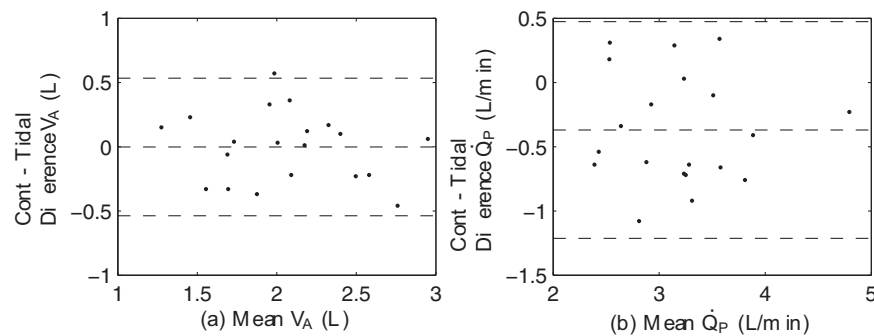


Fig. 4. Comparison of results obtained using the continuous ventilation model with those of the tidal ventilation model, at forcing sinusoidal periods $T=3$ min. Results of V_A and \dot{Q}_P are shown in (a) and (b), respectively, as Bland–Altman plots. The mean and differences (continuous – tidal) of estimates obtained using the two models are shown on the x - and y -axis, respectively. Mean difference and the *limit of agreement* (mean difference $\pm 1.96\sigma$, where σ is the standard deviation of the differences) are plotted as horizontal dashed lines.

Table 1 compares the continuous ventilation model with the tidal ventilation model, using data obtained from a healthy male volunteer. The results in Table 1 are also plotted in Fig. 3(a)–(c), where standard deviations of the results obtained using the proposed tidal ventilation model are shown as error bars. Fig. 3(a)–(c) compares the estimate obtained using the continuous ventilation model with the average values of the estimates produced by the

tidal ventilation model at different forcing frequencies in one individual.

5.2. Results of estimating V_D

Estimated values of V_D using the mean and linear regression approaches are shown in Table 2. Three types of results are

Table 1

Comparison of the continuous ventilation (CV) model with the tidal ventilation (TV) model at different forcing frequencies. Results are obtained from the same healthy male volunteer in Table 2 (age 63 years, height 173 cm, weight 68 kg). V_D results are taken from V_{Dreg} using both CO_2 and N_2O .

T (min)	V_D (L)		V_A (L)		\dot{Q}_P (L/min)	
	CV	TV	CV	TV	CV	TV
2	0.26	0.26	1.77	1.56	2.78	2.11
3	0.26	0.26	1.72	1.66	3.22	3.25
4	0.25	0.25	1.67	1.84	3.54	2.90
5	0.26	0.26	2.55	2.37	2.66	2.29

Table 2

Comparison of V_D estimates obtained using the original Bohr equation with those obtained using our improved Bohr equation. Data were acquired from a healthy male volunteer, age 63 years, height 173 cm, weight 68 kg. Results at different forcing sinusoidal periods T are presented. V_{Davg} is obtained using the averaging approach, and V_{Dreg} is obtained using the proposed linear regression approach.

T (min)	CO_2 only		N_2O only		$\text{CO}_2 + \text{N}_2\text{O}$	
	V_{Davg}	V_{Dreg}	V_{Davg}	V_{Dreg}	V_{Davg}	V_{Dreg}
2	0.27	0.75	0.40	0.26	0.33	0.26
3	0.27	0.65	0.19	0.23	0.23	0.26
4	0.27	0.73	0.26	0.24	0.27	0.25
5	0.27	0.85	0.35	0.24	0.31	0.26

Table 3

Comparison of the continuous ventilation (CV) model with the tidal ventilation (TV) model. Results are obtained from healthy volunteers; the first 13 data sessions are from male volunteers of age 20–60 years, and the remaining 3 data sessions are from female volunteers of age 20–40 years. The standard deviation on the estimates of the TV model are shown as “estimate \pm standard deviation”. Both NO₂ and O₂ are used as indicator gases, and results obtained using NO₂ are shown here. Results obtained using O₂ are similar to those obtained using NO₂, and hence are not shown here. The forcing sinusoidal period $T = 3$ min; V_D estimates are equal to V_{Dreg} using both CO₂ and NO₂.

Session	V_D (L)		V_A (L)		\dot{Q}_P (L/min)	
	CV	TV	CV	TV	CV	TV
1	0.26	0.26 \pm 0.002	1.72	1.66 \pm 0.32	3.22	3.25 \pm 0.85
2	0.28	0.28 \pm 0.001	2.92	2.98 \pm 0.59	3.56	3.46 \pm 0.67
3	0.26	0.26 \pm 0.002	2.69	2.47 \pm 0.43	4.91	4.68 \pm 0.64
4	0.37	0.37 \pm 0.001	1.34	1.57 \pm 0.52	2.38	2.69 \pm 0.62
5	0.33	0.33 \pm 0.001	1.70	2.27 \pm 0.49	3.00	3.29 \pm 0.65
6	0.28	0.28 \pm 0.001	2.99	2.53 \pm 0.31	2.70	2.16 \pm 0.93
7	0.30	0.30 \pm 0.002	1.90	2.26 \pm 0.52	4.09	3.68 \pm 0.69
8	0.32	0.32 \pm 0.002	2.13	2.25 \pm 0.42	4.19	3.43 \pm 0.79
9	0.24	0.24 \pm 0.001	2.35	2.45 \pm 0.38	3.60	2.96 \pm 0.44
10	0.29	0.29 \pm 0.001	2.17	2.18 \pm 0.54	3.91	3.25 \pm 0.72
11	0.23	0.23 \pm 0.001	2.61	2.38 \pm 0.75	3.77	2.85 \pm 0.81
12	0.21	0.21 \pm 0.003	2.24	2.41 \pm 0.36	3.40	3.74 \pm 0.64
13	0.35	0.35 \pm 0.001	2.06	1.69 \pm 0.53	3.19	2.57 \pm 0.42
14	0.25	0.25 \pm 0.002	1.99	2.02 \pm 0.60	3.01	2.84 \pm 0.72
15	0.23	0.23 \pm 0.001	1.72	1.39 \pm 0.47	2.81	2.47 \pm 0.82
16	0.29	0.29 \pm 0.001	2.20	1.98 \pm 0.34	2.44	2.62 \pm 0.52
17	0.27	0.27 \pm 0.002	1.86	1.53 \pm 0.46	2.71	2.07 \pm 0.71
18	0.23	0.23 \pm 0.001	1.20	1.35 \pm 0.51	3.35	2.27 \pm 0.73
19	0.22	0.22 \pm 0.003	1.79	2.12 \pm 0.61	3.61	2.89 \pm 0.59
20	0.27	0.27 \pm 0.001	1.71	1.75 \pm 0.34	3.59	2.88 \pm 0.75

presented: results obtained using CO₂, results obtained using N₂O, and results obtained using both CO₂ and N₂O. Results obtained using indicator gas O₂ are similar to those using N₂O, and are not shown here.

5.3. Results from all human volunteers

Fig. 4 shows V_A and \dot{Q}_P results from all human volunteers. Table 3 compares the results derived from the continuous model with the tidal ventilation model. Results of V_D , shown in Table 3, obtained using the continuous model are, with experimental error, the same as those obtained using the tidal model. Hence, they are not plotted in Fig. 4.

6. Discussion

It is acknowledged that the two models described in this work have only a single alveolar compartment and a single dead space compartment. The great advantage of these models is that they can be “inverted” when real physiological data is inserted in them to reveal estimates of physiological variables which have meaning to the clinician or physiologist. Due to their simplicity, they can only be used to describe relatively healthy lungs. However, as Whiteley et al. (Whiteley et al., 2000) demonstrated, the use of mathematical models with more than one lung compartment can lead to great difficulty in reaching an inverse solution for the respiratory variables of dead space, alveolar volume, and pulmonary blood flow when the subject’s lung is inhomogeneous. Also, such models do not lend themselves readily to physiological interpretation. This is why simple one-alveolar lung compartment models have survived the succeeding decades after they were first proposed (Hahn and Farmery, 2003). Our techniques are likely to be valid in exercise testing in subjects or patients without overt lung disease, and could be applied to the field of human exercise physiology, as pioneered by Luijendijk et al. (Luijendijk et al., 1981) for the forced inspired sine wave technique.

We have not yet evaluated the techniques for patients with severe lung disease. However, we note that for our single compartment model, the solutions for V_A , V_D , and \dot{Q}_P should be the same regardless of the period of the sinusoid. Our preliminary modelling and experimental work reveals that where ventilatory inhomogeneity exists, the determined variables appear to be dependent on the period. The degree of period dependency is likely to provide a robust index of ventilatory heterogeneity, and this will be developed in future work.

Oxygen is used as an indicator gas in these studies. It is assumed that oxygen behaves much like an insoluble inert gas with respect to the diminution of the amplitude of its sinusoidal inspired concentration within the alveolar compartment. This is because in this analysis it is only the oscillatory components of the indicator concentration signal which is required for the analysis. The static or “DC” component of the signal can then be neglected. This was described in detail by Hahn (1996). The effect is independent of arterial oxyhaemoglobin saturation and concentration and there is no recirculation of the oscillatory signal in the venous blood.

6.1. Comparison of the continuous ventilation model with the tidal ventilation model

Fig. 3(a)–(c) shows the estimates for V_A , \dot{Q}_P , and V_D obtained using the continuous ventilation and the tidal ventilation model at different forcing periods. It can be seen that the estimates of \dot{Q}_P obtained using both the continuous ventilation model and the tidal ventilation model are similar for all forcing sinusoidal periods $T = 2, 3, 4, 5$ min. Similar behaviour can be observed in the estimates of V_A at $T = 2, 3, 4$ min where the estimates of V_A are close to the expected value, but V_A estimates differ from expected values when $T = 5$ min. This may be due either to potential artifact from “venous recirculation”, or to the fact that the recovered values become frequency dependent if real data from inhomogeneously ventilated lungs are analysed in a single compartment model. The consistency of the results using both the continuous ventilation model and the tidal ventilation model for $2 \leq T \leq 4$ suggests that this range is suitable for the forcing sinusoid. For both the continuous ventilation model and the tidal ventilation model, V_D is calculated by the proposed regression method using both CO₂ and NO₂ as described in Section 4. The results of V_D estimation are the same for both models, and are close to the expected value (0.25 L), indicating that the proposed improved Bohr equation method produces stable estimation of V_D .

However, we note that the estimated values of \dot{Q}_P appear smaller than the expected value of \dot{Q}_P of the volunteer (4.5 L/min). One possible reason is that the effect of “venous recirculation” of the N₂O still exists to some degree, whereas both the continuous ventilation model and the tidal ventilation model assume that it is negligible. Another possible reason is that the equilibrium between the arterial and venous blood had not yet been established during the data collection, although nitrous oxide has low blood and tissue solubility. In this early stage of the pilot study on human volunteers, we did not use a comparator for \dot{Q}_P , but our results have shown that the proposed tidal ventilation model is able to produce consistent and repeatable results. In the next stage of the study, we will incorporate a comparator algorithm, further investigate “venous recirculation” and ventilatory inhomogeneity, and ensure that the complete equilibrium of nitrous oxide is established for data collection.

6.2. Results of V_D

Estimated values of V_D using the mean and linear regression approaches are shown in Table 2. Using only CO₂, the mean approach produces more consistent estimates of V_D than regression

at all forcing sinusoidal periods T . By contrast, when using only N_2O , estimates of V_D using regression are more stable than those obtained using the mean. The reason for such behaviour is demonstrated in Fig. 3(d), where the (x, y) pairs in (30) for CO_2 form a dense cluster, while the (x, y) pairs for N_2O resemble a straight line.

6.3. Results from all human volunteers

Fig. 4(a) shows that the differences in V_A estimates obtained from the tidal and continuous ventilation models have a mean difference of approximately zero, and differences about this mean are not correlated with the mean of the estimates.

While differences in the estimates of \dot{Q}_P obtained from both models are similarly uncorrelated to the means of the estimates, Fig. 4(b) shows that the mean difference is approximately -0.35 L/min; i.e., the estimate obtained from the continuous model is an average of 0.35 L/min lower than that obtained from the tidal model.

Table 3 shows the results of using each model for estimating V_D , V_A and \dot{Q}_P . As described earlier, the tidal ventilation model takes an approach whereby the data acquired in a session are divided into a set of 20 windows, with an estimate of lung variables provided for each window. The table reports the mean and standard deviation of this set of 20 estimates for the tidal ventilation model, for each session. The continuous ventilation model, however, uses all of the data from a session to produce a single estimate of each lung variable; therefore, the table reports only these single estimates (i.e., without standard deviation) for the continuous ventilation model.

7. Conclusion

The continuous ventilation model uses only the amplitude of indicator gas concentration, without incorporating other variables, hence the underlying physiological information may not be sufficiently characterised. In comparison, a tidal ventilation model allows the examination of the effect of V_D , V_A , respiratory rates, etc. (Hahn and Farmery, 2003); therefore variations in variables can be more accurately investigated.

The proposed tidal ventilation model is able in theory, with noise-free data, to estimate lung variables using two successive breaths. In practice, it is desirable to use a few more than two breaths for robust estimation for on-line patient monitoring. This procedure is much faster than using the traditional continuous ventilation model, which requires a relatively long data collection time (at least two forcing periods). On the other hand, the tidal ventilation model is marginally more sensitive to measurement error. However, the output of the continuous ventilation model produces a stable single set of estimates for a certain duration, and this could be used as a check against the output of the tidal ventilation model.

The proposed improved Bohr equation method produces stable estimates of V_D . Results using both the continuous ventilation model and the tidal ventilation model have shown that $2 \leq T \leq 4$ is a potentially suitable range for the forcing sinusoid, in order to achieve reliable variable determination and to avoid recirculation effects. The proposed experimental gas delivery technique is suitable for use in assessing lung function in patients with healthy lungs in the clinical setting, and in exercise physiology, but further testing is needed to further validate the algorithm that we have used.

Acknowledgements

The authors gratefully acknowledge funding by EPSRC (grant number EP/E028950/1). LC was supported by the Overseas Research Students Award Scheme, provided by the UK Government, and is currently supported by the NIHR Biomedical

Research Centre Programme, Oxford. DAC was supported by the Wellcome Trust/EP SRC Centre of Excellence in Personalised Healthcare (grant number WT 088877/Z/09/Z). The authors give sincere thanks to Roger Belcher and Lionel Gale for their valuable technical assistance.

Appendix A. List of abbreviations

The abbreviations used in this paper are summarised as follows:

V_A	lung volume at the end of expiration
V_D	airway dead space volume
V_I	volume of the indicator gas delivered into the lung during a breath
V_E	expired volume of the indicator gas during a breath
V_Q	uptake of the indicator gas during a breath
$\dot{V}(t)$	respiratory flow rate at time t
$F_{IA,n}(t)$	inspired indicator gas concentration in the lung during breath n
$F_{A,n}$	indicator gas concentration in the lung during breath n
$F_{I,n}(t)$	indicator gas concentration during inspiration of breath n
$F_{E',n}$	indicator gas concentration at the end of expiration in breath n
$V_{T,n}$	tidal volume of breath n
λ_b	tissue-gas partition coefficient of a gas
\dot{Q}_P	pulmonary blood flow through the lung
F_A	indicator gas concentration in the lung
\bar{F}_E	average measured indicator gas concentration during expiration
F_I'	indicator gas concentration at the end of inspiration
F_E'	indicator gas concentration at the end of expiration

References

- Clifton, L.A., Farmery, A.D., Hahn, C.E.W., 2009. A non-invasive method for estimating lung function. In: IET Condition Monitoring, Dublin, Ireland, pp. 509–518.
- Farmery, A.D., 2008. Interrogation of the Cardiopulmonary System with Inspired Gas Tension Sinusoids.
- Farmery, A.D., Hahn, C.E.W., 2000. Response-time enhancement of a clinical gas analyzer facilitates measurement of breath-by-breath gas. *Journal of Applied Physiology* 89 (2), 581–589.
- Fletcher, R., Jonson, B., Cumming, G.S.B.J., 1981. The concept of deadspace with reference to the single breath test for carbon dioxide. *British Journal of Anaesthesia* 53, 77–81.
- Fowler, W.S., 1948. Lung function studies II. *American Journal of Physiology* 154, 405–416.
- Gavaghan, D.J., Hahn, C.E.W., 1995. A mathematical evaluation of the alveolar amplitude response technique. *Respiration Physiology* 102 (1), 105–120.
- Gavaghan, D.J., Hahn, C.E.W., 1996. A tidal breathing model of the forced inspired inert gas sine-wave technique. *Respiration Physiology* 106 (2), 209–221.
- Hahn, C.E.W., 1996. Oxygen respiratory gas analysis by sine-wave measurement: a theoretical model. *Journal of Applied Physiology* 81 (2), 985–997.
- Hahn, C.E.W., Black, A.M., Barton, S.A., Scott, I., 1993. Gas exchange in a three-compartment lung model analyzed by forcing sinusoids of N_2O . *Journal of Applied Physiology* 75 (4), 1863–1876.
- Hahn, C.E.W., Farmery, A.D., 2003. Gas exchange modelling: no more gills, please. *British Journal of Anaesthesia* 91 (1), 2–15.
- Hamilton, R.M., 1998. *Cardiorespiratory Measurements Using Inspired Oxygen Sinewaves*.
- Hlastala, M.P., Berger, A.J., 1996. *Physiology of Respiration*, 1st ed. Oxford University Press, Oxford.
- Luijendijk, S.C.M., Zwart, A., van der Kooij, A.M., de Vries, W.R., 1981. Evaluation of alveolar amplitude response technique for determination of lung perfusion in exercise. *Journal of Applied Physiology* 50 (5), 1071–1078.
- Rouby, J.J., Constantin, J.M., Girardi, C.d.A., Zhang, M., Lu, Q., 2004. Mechanical ventilation in patients with acute respiratory distress syndrome. *Anesthesiology* 101, 228–234.
- Sainsbury, M.C.A.L., Williams, E.M., Hahn, C.E.W., 1997. A reconciliation of continuous and tidal ventilation gas exchange models. *Respiration Physiology* 108 (1), 89–99.
- Van der Hoeven, S.W., 2007. *Modelling and Control of Gas Flow in Anaesthesia*.
- Whiteley, J.P., Farmery, A.D., Gavaghan, D.J., Hahn, C.E.W., 2003. A tidal ventilation model for oxygenation in respiratory failure. *Respiration Physiology* 136 (1), 77–88.

- Whiteley, J.P., Gavaghan, D.J., Hahn, C.E.W., 2000. A tidal breathing model of the inert gas sinewave technique for inhomogeneous lungs. *Respiration Physiology* 124 (1), 65–83.
- Williams, E.M., Aspel, J.B., Burrough, S.M., Ryder, W.A., Sainsbury, M.C., Sutton, L.L.X., Black, A.M., Hahn, C.E.W., 1994. Assessment of cardiorespiratory function using oscillating inert gas forcing signals. *Journal of Applied Physiology* 76 (5), 2130–2139.
- Williams, E.M., Sainsbury, M.C., Sutton, L., Xiong, L., Black, A.M.S., Whiteley, J.P., Gavaghan, D.C., Hahn, C.E.W., 1998. Pulmonary blood flow measured by inspiratory inert gas concentration forcing oscillations. *Respiration Physiology* 113 (1), 47–56.
- Zwart, A., Bogaard, J.M., Jansen, J.R.C., Versprille, A., 1978. A non-invasive determination of lung perfusion compared with the direct Fick method. *Pfawers Archiv European Journal of Physiology* 375 (2), 213–217.
- Zwart, A., Seagrave, R.C., van Dieren, A., 1976. Ventilation-perfusion ratio obtained by a noninvasive frequency response technique. *Journal of Applied Physiology* 41 (3), 419–424.